The lowest nπ* states of heteroaromatics: When and in what way are they aromatic or antiaromatic?

Nathalie Proos Vedin,[a] Sílvia Escayola,[b,d] Slavko Radenković,[c]* Miquel Solà,[b]* and Henrik Ottosson [a]*

[a] Department of Chemistry - Ångström Laboratory, Uppsala University, 751 20 Uppsala, Sweden. [b] Institut de Quìmica Computacional i Catàlisi and Departament de Quìmica, Universitat de Girona, C/ Maria Aurèlia Capmany, 69, 17003 Girona, Catalonia, Spain. [c] University of Kragujevac, Faculty of Science, P. O. Box 60, 34000 Kragujevac, Serbia. [d] Donostia International Physics Center (DIPC), 20018 Donostia, Euskadi, Spain.

Abstract: Heteroaromatic molecules are ubiquitous and found in many areas of chemistry, ranging from biochemistry to organic electronics. Herein we analyse the nπ* excited states of $(4n+2)\pi$-electron heteroaromatic compounds that have in-plane lone-pair orbitals (n_σ, here labelled n), using both qualitative theory and quantum chemical computations. The starting point of our analysis is Mandado's $2n+1$ rule for aromaticity of separate spins. After excitation of an electron from n to π* a $(4n+2)\pi$-electron species will have $2n+2$ π_α-electrons and $2n+1$ π_β-electrons (or *vice versa*), and thus would be π_α-antiaromatic and π_β-aromatic. We ask, does this lead to a nonaromatic nπ* state? We show that the situation is complex as the antiaromatic π_α- and the aromatic π_β-components often do not cancel, leading to residuals which either lean towards aromaticity or antiaromaticity. Focus is placed on the vertically excited nπ* states with triplet multiplicity as they are most readily analysed, yet we also explore singlet nπ* states.

Pyrazine and the phenyl anion are examples of molecules with residuals in their $n\pi^*$ states which are markedly aromatic. We seek and provide qualitative explanations as to which compounds have $n\pi^*$ states with residuals which are aromatic in character, and which ones are antiaromatic. Our results show that if the π_β-electron population becomes more uniformly distributed in the excitation, the system will have an aromatic residual and *vice versa*. For isomeric species, the isomer with the most aromatic residual in $^3n\pi^*$ is often of lowest relative energy in this state. Finally, we connect our findings to the recently observed adaptive aromaticity phenomenon, especially found in some metallaaromatics, and show that it can be understood with the general theoretical framework described herein.

Introduction

Heteroaromatic compounds are central to a number of areas of chemistry and related fields, including pharmaceutical chemistry, biochemistry, agrochemistry, organic electronics, and photovoltaics.[1-8] It has been estimated that two thirds of the ~20 million compounds that were known at the end of last century are aromatic or have aromatic parts, and that about half are heteroaromatics.[1] Thus, it is broadly important to understand their electronic structures, and this applies to both their singlet ground states (S_0) and first electronically excited states of singlet and triplet multiplicity (S_1 and T_1). One important characteristic is their extent of (anti)aromaticity, and in the lowest $\pi\pi^*$ excited states, (anti)aromaticity is often given by Baird's rule.[9-17] This rule tells that annulenes with $4n$ π-electrons are aromatic while those with $4n+2$ are antiaromatic in their lowest $\pi\pi^*$ states. Yet, this form of excited state (anti)aromaticity is not valid to heteroaromatics with $n\pi^*$ states as their lowest excited states, *e.g.*, pyridine and pyrazine. Now, how to assess and rationalize the potential aromatic or antiaromatic character of the $n\pi^*$ states of heteroaromatic compounds?

A heteroaromatic molecule with six π-electrons in the S_0 state (three π_α and three π_β) will in its $n\pi^*$ state, when n is an in-plane orbital, have four π-electrons of one spin and three of the other, and this is the case for both the singlet and triplet $n\pi^*$ state (Figure 1A). To understand their aromatic, non-aromatic or antiaromatic characters, we now utilize Mandado's $2n+1$ rule for aromaticity of separate spins.[18] With this rule, Hückel's $4n+2$ rule for closed-shell singlet state aromaticity can be fractioned into $2n+1$ π_α-electron and $2n+1$ π_β-electron parts (Figure 1B), while Baird's $4n$ rule for the lowest $\pi\pi^*$ triplet state of [$4n$]annulenes can be fractioned into $2n+1$ π_α-electrons and $2n$-1 π_β-electrons, both numbers corresponding to aromaticity for separate spins. Conversely, the T_1 state of a species with $4n+2$ π-electrons can be described as antiaromatic, having $2n+2$ π_α- and $2n$ π_β-electrons. A similar rule reported by Valiev *et al.* considers that molecules are aromatic (or antiaromatic) if they have an odd (or even) number of doubly and singly occupied π-conjugated valence orbitals,[19] suggesting that Mandado's rule can be expanded to the singlet excited state with the same electron configuration as the $\pi\pi^*$ T_1 state.

The situation becomes more complex in heteroaromatics with in-plane lone-pairs (n_σ, hereafter labelled n). The $n\pi^*$ state of such a $(4n+2)\pi$-electron heteroaromatic molecule has $2n+2$ π_α- and $2n+1$ π_β-electrons (or *vice versa*), and would at first glance be nonaromatic as the aromatic π_β-component will be cancelled by the antiaromatic π_α-component. Yet, is it that simple? Can the combination of the two parts instead lead to a residual which leans towards aromaticity or antiaromaticity if one of the components is stronger than the other? If so, for which molecules is that the case?
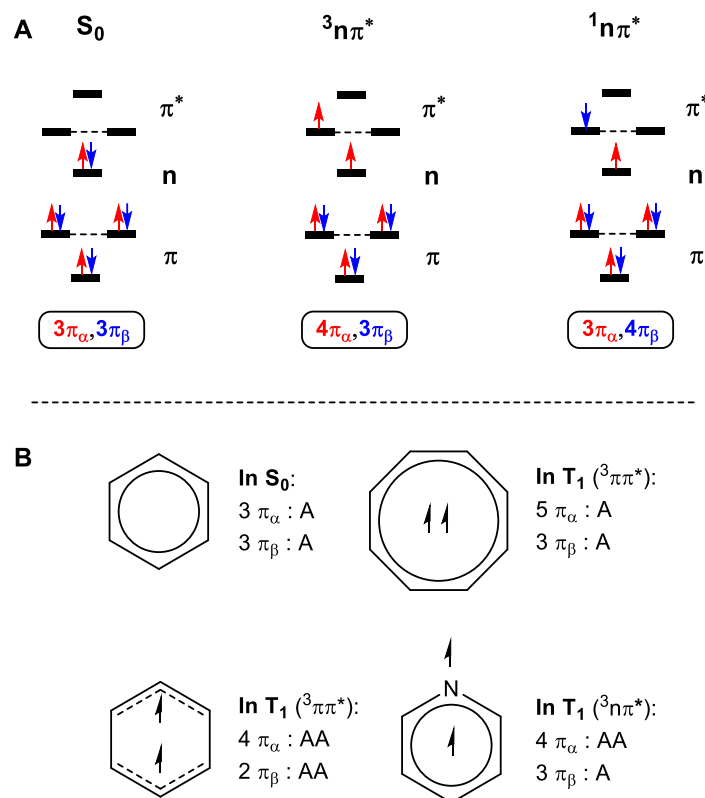
A **S₀**

S_0 $^3n\pi^*$ $^1n\pi^*$

$3\pi_\alpha, 3\pi_\beta$ $4\pi_\alpha, 3\pi_\beta$ $3\pi_\alpha, 4\pi_\beta$

B

In S_0:
3 π_α : A
3 π_β : A

In T_1 ($^3\pi\pi^*$):
5 π_α : A
3 π_β : A

In T_1 ($^3\pi\pi^*$):
4 π_α : AA
2 π_β : AA

In T_1 ($^3n\pi^*$):
4 π_α : AA
3 π_β : A

Figure 1: (A) Orbital occupancies in the S_0 state (n^2) and the triplet and singlet $n\pi^*$ states, with α-electrons in red and β-electrons in blue. (B) Illustrations of Mandado's rule for (anti)aromaticity of separate spins with aromaticity (A) and antiaromaticity (AA) components in the S_0 and T_1 ($\pi\pi^*$) states of benzene, the T_1 ($\pi\pi^*$) state of cyclooctatetraene, and the T_1 ($n\pi^*$) state of pyridine.

Although the (anti)aromatic characters of various heteroaromatics in their lowest excited states have been analyzed earlier through computations,[20,21] the (anti)aromaticity of the $n\pi^*$ states of various heteroaromatics has not been addressed earlier, neither through qualitative theory nor quantitative computations. We argue that such information can be important to rationalize fundamental characteristics of $n\pi^*$ states; what are the implications of an aromatic residual for the excited state properties of heteroaromatics in their lowest $n\pi^*$ states? We hypothesise that compounds with $n\pi^*$ states with aromatic residuals may have these states as

their lowest excited states, with lower excitation energies and higher photochemical stabilities than (isomeric) compounds with nπ* states having nonaromatic or antiaromatic residuals.

In this context, one can note the recently introduced concept of adaptive aromaticity observed through computations of some metallaaromatic compounds.[22-25] The lowest excited states of these species are often of πσ* or σπ* character, *i.e.*, states which also have differences of one electron in the π_α- *versus* π_β-electron counts. Situations with residuals between the two spin components that lean towards aromatic character may be found also in some of these species in their πσ* and σπ* states. If so, this would provide for a deeper rationalization of the adaptive aromaticity phenomenon as observed in the metallaaromatic species.

The extent of aromaticity in the S_0 state of many heteroaromatic compounds has already been reported in earlier studies.[26,27] The compounds which we now investigated in their nπ* states are displayed in Figure 2, and they are grouped so as to allow us to explore the effects of ring-size, heteroatom electronegativity, number of heteroatoms, and their relative positions. Group A consists of six-membered ring heterocycles with one heteroatom (labelled E) each. Although the phenyl anion and dianions (**3**, **17** and **18**) strictly are not heterocycles, we consider the sp^2 hybridized carbon atoms with in-plane lone-pairs as heteroatoms. Thus, even though most of the compounds are common heterocycles, we also included species which are less abundant as they allow us to explore a wider span in the choice of heteroatoms, ring-size, and placement of the heteroatoms, thereby making general trends more apparent. Noteworthy, we focus on heteroaromatics with nπ* states among the lowest few excited states, whereby they are photochemically relevant. Therefore, we did not consider five-membered ring heteroaromatics such as furan, thiophene, and imidazole as these species have nπ* states of very high energies placed well above their lowest ππ* (and even Rydberg) states. Due to the high $E(n\pi^*)$ and the complicated nature of these nπ* states, which are not easily observed

experimentally,[28] we discuss these heteroaromatics only in the Supporting Information (section 3.5).

As will be shown, by considering the residuals between the two spin components of (anti)aromaticity we can rationalize features of the heteroaromatics in their $n\pi^*$ states. For example, why there is an energetic drive for perfluoropyridazines to photorearrange to the corresponding pyrazines, as has been observed experimentally and concluded to proceed in the singlet $n\pi^*$ state.[29,30] Hence, we provide a general framework for the rationalization of the (anti)aromatic character of $n\pi^*$ states of common heteroaromatics found throughout chemistry.
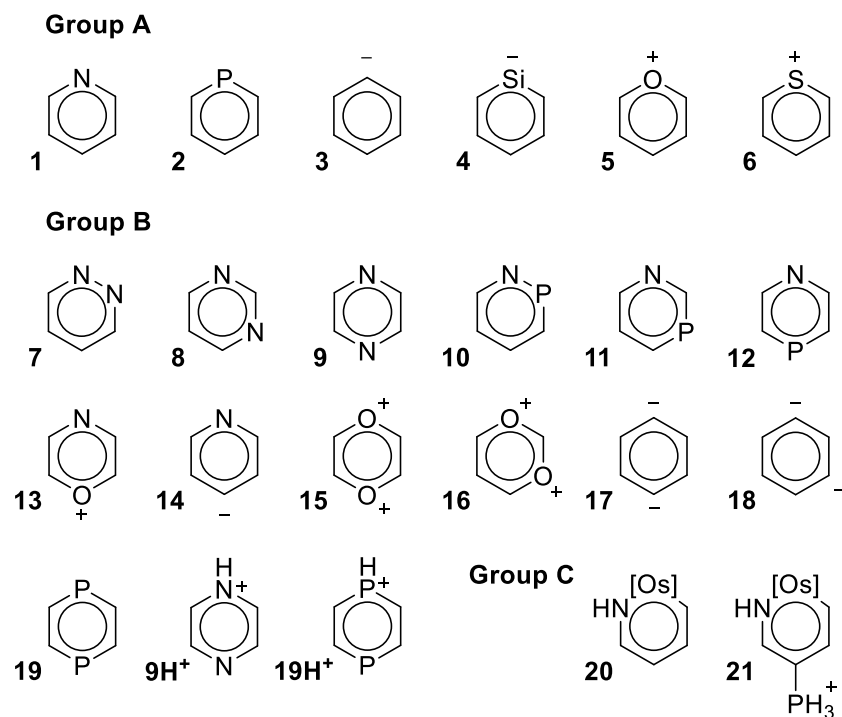

Figure 2: The compounds and groups investigated herein. [Os] = $OsCl_2(PH_3)_2$.

Qualitative Theory

Before discussing the computational results, we describe the qualitative molecular orbital (MO) theoretical framework which our analysis relies upon. We foremost explore the vertical excitation because in the vertically excited $n\pi^*$ state the π_β-component should, viewed simplistically based on Figure 1A, remain as aromatic as in S_0, while the π_α-component with

four π_α-electrons should be antiaromatic in character. Yet, is this the case? Factors that may perturb this simplistic description of the aromaticity of the nπ* state are (*i*) a difference in electrostatics within the π-orbital frameworks of the S$_0$ and nπ* states as there will be an increased Coulomb repulsion in the π-system because of the additional π-electron in the nπ* state, and (*ii*) a difference in the exchange interaction resulting from the difference in the number of π_α- and π_β-electrons. A residual that tends towards aromaticity of a vertically excited nπ* state of a heteroaromatic compound will result if there is (*i*) a higher degree of aromaticity in the π_β-component compared to the S$_0$ state and/or (*ii*) a low degree of antiaromaticity in the π_α-component. Similarly, a compound can have a residual that tends toward antiaromaticity due to a lower aromaticity in the π_β-component than in S$_0$ and/or a high degree of antiaromaticity in the π_α-component.

Next, when the molecule relaxes from the vertically excited nπ* state one can postulate that there will be a tug-of-war between the aromatic π_β-component that should seek to retain the (planar) S$_0$ state geometry and the antiaromatic π_α-component that should seek to alleviate its antiaromatic character by driving the molecule towards a distorted structure (Figure 3A), *i.e.*, a more bond length alternated and/or puckered structure. Thus, if the residual between the π_α- and π_β-(anti)aromaticity components corresponds to some aromatic character we postulate that the molecule will be more prone to retain a planar and bond length equalized structure in the nπ* state, while it will pucker and/or become more bond length alternated if it has a residual with some antiaromatic character. Yet, there can be factors that counteract these features, such as the preference for a particular heteroatom to have a more acute bond angle than allowed in the planar structure. Hence, by jointly regarding the aromatic-antiaromatic character of the vertically excited nπ* state, we can probe the hypothesis that molecules with

nπ* states with aromatic residuals between the π_α and π_β components will distort less while those with antiaromatic residuals will distort more.
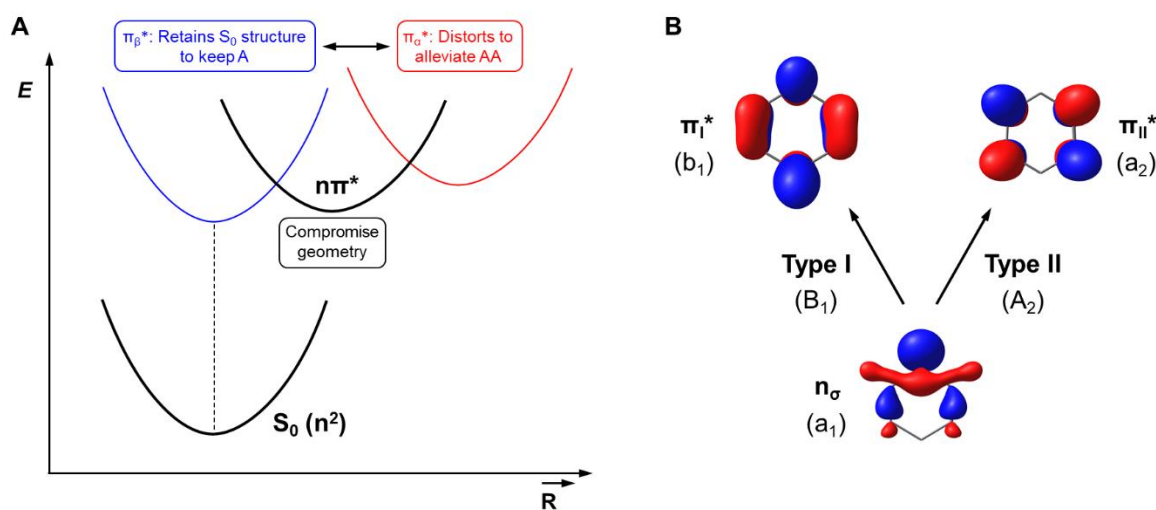

Figure 3: (A) Illustration of the tug-of-war between the aromatic (A) π_β-component and the antiaromatic (AA) π_α-component in influencing the structure of the nπ* state. (B) The two general types of nπ* excitations for a molecule with C_{2v} symmetry that can be the lowest nπ* state, and the orbital and state symmetries.

There are also various types of nπ* states with different state symmetries as there are two π* orbitals (the b_1 and a_2 orbitals, Figure 3B), which are degenerate in benzene. As the b_1 π* orbital has a lobe at the E atom while the a_2 π* orbital has a node, it is apparent that the orbital energy gap and the energies of the two nπ* states should be affected differently by the electronegativity of the E atom.

With several heteroatoms (E and E') with in-plane lone-pair electrons the situation becomes more complex because the excitation can be out of either the in-phase or the out-of-phase combination of the localized n(E) and n(E') orbitals. Throughout we focus on the lowest nπ* state, yet in a few cases we explored also the second lowest in order to establish an unambiguous comparison between analogous nπ* states of the heteroaromatic compounds in a

particular Group. Moreover, the lowest $^3n\pi^*$ state is not necessarily the T_1 state as the lowest state instead can be of $\pi\pi^*$ or Rydberg character. We found that six-membered ring (6-MR) heteroaromatics often have T_1 states of $n\pi^*$ or $\pi\pi^*$ character, while the T_1 state of five-membered ring (5-MR) heteroaromatics (as noted above) mainly are of π to Rydberg character as the in-plane n orbitals are of low energy and the π^* orbitals are of high energy when compared to the 6-MR heteroaromatics (see section 3.5 of the Supporting Information for a further analysis).

Results and Discussion

The heterocycles investigated are analysed following the groups shown in Figure 2, with the most thorough analysis of Group A. We primarily explored the $^3n\pi^*$ state as it allows us to use a larger portfolio of aromaticity descriptors, yet, we also calculated several compounds in their $^1n\pi^*$ states to probe whether the trends in (anti)aromatic character are the same for singlet and triplet $n\pi^*$ states. Computations for the $^3n\pi^*$ states were mainly performed with the long-range corrected CAM-B3LYP functional[31] in the unrestricted Kohn-Sham (KS) formalism, but calculations with the B3LYP and BLYP functionals[32,33,34] as well as CCSD, BD, and CASSCF were performed for selected compounds (see sections 2.1, 3.1 and 3.4 of the ESI). Recently, the performance of the CAM-B3LYP, ωB97X-D, and M06-2X functionals were explored for the lowest excited states of benzene, pyridine, and the three diazines, and it was concluded that the long-range corrected CAM-B3LYP and ωB97X-D functionals give the best results.[20] For the $^1n\pi^*$ states, we used time-dependent (TD) DFT. Emphasis is placed on electronic indices, although for Groups A and C and selected Group B heteroaromatics, we also analysed the spin-separate magnetically induced current densities (MICDs). For the $^3n\pi^*$ states, we analysed geometry-based parameters and computed the relaxation energies when going from the vertically excited to the relaxed $^3n\pi^*$ states; do they reflect the drive to relieve antiaromatic

character of the π_α-component of the $n\pi^*$ state or the strive of the π_β-component to retain aromaticity?

Assessment criteria: Among electronic indices we computed (spin-separated) multicenter indices (MCI) and electron density of delocalized bonds (EDDB) values,[35,36,37,38] with focus on the MCI results. Here it should be noted that the σ-contributions to the MCI values are negligible (less than 2% in almost all systems and up to 5% and 7% for the $^3n\pi^*$ states of **6** and **12**, respectively), except for the $^3n\pi^*$ states of **5**, **15**, and **16** for which the MCI_σ (basically $MCI_{\sigma\beta}$) represent up to 25-30% of the total MCI (see Table S18). It is worth noting that S_0 states of **5**, **15**, and **16** are nonaromatic and, therefore, the MCI_σ contributions do not modify the conclusion about the lack of aromaticity of these $^3n\pi^*$ states. We explored for which compounds the MCI_β components of the $^3n\pi^*$ states are smaller than in S_0 (*i.e.*, half of the total MCI in S_0), and for which compounds this component is larger. The MCI_α-component will decrease to a very low value as it becomes antiaromatic, yet its antiaromatic character cannot be assessed as easily as the aromatic character of the MCI_β-component, and it is not analysed as extensively. The residual is what results when the MCI_α- and MCI_β-components have been summed together; for an $n\pi^*$ state which is nonaromatic, the MCI value should be close to half the total value in S_0 as the MCI_α-component will be nearly zero while the MCI_β-component remains as in S_0. We consider the residual of an $n\pi^*$ state to lean towards aromaticity if the combined MCI_α and MCI_β components are at least 10% higher than half the total MCI value of S_0, and towards antiaromaticity if 10% lower.

For the S_0 state, we consider a 6-MR molecule to be aromatic if its MCI value is at least half the MCI value of benzene in S_0 (*i.e.*, $0.0716/2 = 0.0358$). Yet, the vertically excited lowest triplet $\pi\pi^*$ states of this species has multiconfigurational character and are therefore not (easily) comparable to those of the lower-symmetry heterocycles. Instead, the MCI and EDDB

values of the lowest $^3\pi\pi^*$ state of pyridine was used as this state is single-configurational and also antiaromatic in both α- and β-components according to Mandado's rule. Thus, this state serves as an antiaromatic reference state with a total MCI value of -0.0005, and α- and β-spin components of 0.0023 and -0.0028, respectively.

In the (anti)aromaticity assessments of the $n\pi^*$ states of a compound, we therefore use the following two criteria; (*i*) the ratio between the total MCI in the $n\pi^*$ state and that of the S_0 state of the specific compound, and (*ii*) a comparison of the S_0 state of a specific heteroaromatic against the aromaticity of benzene in S_0 (aromatic reference) and the antiaromaticity of the triplet $\pi\pi^*$ states of pyridine (antiaromatic reference).

Monoheteroaromatic 6-MRs (Group A): As postulated above, the split between the two π^* orbitals, b_1 and a_2, becomes gradually larger as the electronegativity of the heteroatom E increases with a more marked lowering of the b_1 orbital energy. The 1^3B_1 is the lowest $^3n\pi^*$ state for all Group A compounds, yet, the energy difference to the other $^3n\pi^*$ state (1^3A_2) is merely 0.20 eV for **3** while it is 2.05 eV for **5**. With regard to the singlet $n\pi^*$ states, all Group A heteroaromatics except **3** have 1^1B_1 states as the lowest. For **3**, the energy gap is reversed but with 1^1A_2 below 1^1B_1 by merely 0.42 eV. It should, however, be noted that the triplet $n\pi^*$ states of **5** and **6** have multireference character as they have T_1 diagnostic values of, respectively, 0.060 and 0.045, *i.e.*, higher than the threshold 0.044 for open-shell species.[39,40,41] Yet, despite their multiconfigurational character, the ratios between the MCI values in the triplet $n\pi^*$ and S_0 states of **5** and **6** obtained from the (U)CAM-B3LYP, (U)CCSD, and (U)BD methods are quite similar (see Tables S1, S4 and S5), showing that the (U)CAM-B3LYP method can produce reliable estimates of the decreases in aromaticity when going from S_0 to the $n\pi^*$ states of these species.

When evaluated based on our definition of the residual, the $^3n\pi^*$ state of the phenyl and silaphenyl anions (**3** and **4**) have residuals with MCI that lean towards aromaticity;

their MCI_β-components are significantly higher than the corresponding values in the S_0 state (Figure 4A), and the MCI_α-components are similar to that of pyridine in its lowest $^3\pi\pi^*$ state (0.0026 and 0.0011 vs. 0.0023, respectively). Interestingly, the relative increase in the aromatic character of the MCI_β-component is larger in **4** than in **3**. In contrast, the lowest $^3n\pi^*$ states of pyridine (**1**) and the thiopyrylium cation (**6**) have residuals that lean towards antiaromaticity, while for phosphinine (**2**) the MCI_β-component of its $^3n\pi^*$ state is very similar to that of S_0 and it should be categorized as nonaromatic. In S_0, the pyrylium cation (**5**) has an MCI value which is lower than the threshold for aromaticity (0.0358) and we label it as nonaromatic in this state. However, in its first $^3n\pi^*$ state, the MCI_β-component of **5** is somewhat higher (in part because of its non-negligible MCI_σ contribution), although it is still the lowest among the Group A compounds. Thus, it should be justified to label **5** as nonaromatic also in its $^3n\pi^*$ state. With regard to the MCI_α-components in the lowest $^3n\pi^*$ states of Group A compounds, it is notable that they are similar or only slightly higher (0.0011 – 0.0030) than in the corresponding antiaromatic $^3\pi\pi^*$ state of these compounds (MCI_α-component with four electrons are in the range -0.0012 – 0.0034).
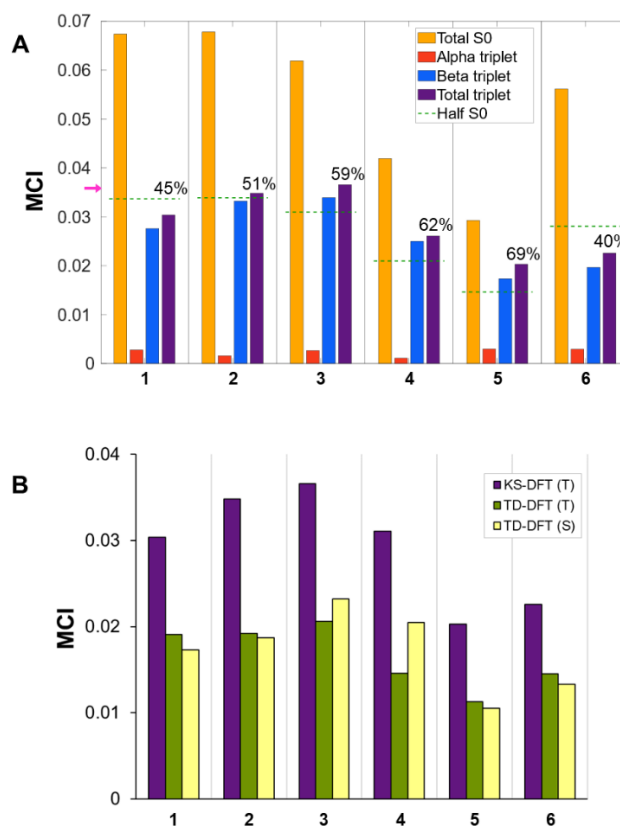
Figure 4: The MCI results (in atomic units) of Group A heteroaromatics in (A) their nπ* triplet states (spin-separated MCI) with KS-UDFT, and (B) MCI results at TD-DFT level for triplet and singlet nπ* states as well as the KS-UDFT results for the ^{3}nπ* states for comparison. A purple arrow in panel A indicates half the MCI value of S_0 benzene, *i.e.*, our aromaticity threshold.

For the lowest singlet nπ* states, we used TD-DFT for which spin-separation is not possible. Therefore, to assess the results from TD-DFT, as compared to those from KS-DFT, we computed excitation energies and MCI values for the triplet nπ* states using both formalisms and found that MCI values from TD-DFT are consistently lower by a third to half the values from KS-UDFT (Figure 4B). Despite this, the trends observed in the TD-DFT results for the lowest ^{3}nπ* states are very similar to those of KS-UDFT presented above, both in terms

of excitation energies and relative (anti)aromaticity assessed by MCI. Thus, we are confident that we can explore the $^1n\pi^*$ and $^3n\pi^*$ states on comparable footings.

The energetic order of the vertically excited $^1n\pi^*$ states matches well that of the corresponding $^3n\pi^*$ states, and the calculated total MCI values show that the (anti)aromatic characters in the two states are very similar for most compounds of Group A. The exceptions are **3** and **4** for which the singlet $n\pi^*$ states are more aromatic than the triplets and differ to a higher degree than for the other compounds. Yet, an unambiguous analysis of the cause of this difference cannot be made as it is not possible to separate the MCI_α- and MCI_β-components in results from TD-DFT computations. Still, for **4** we observe that the lowest $^1n\pi^*$ state (the S_2 state) is of mixed $n\pi^*$/Rydberg character in contrast to the $^3n\pi^*$ states which are pure valence excited states. On the other hand, for **3** the first $^1n\pi^*$ state is an A_2 state (Type II, Figure 3B) in contrast to the other Group A compounds where these states are of B_1 symmetry. Despite these two exceptions, in most cases the extent of (anti)aromaticity of the lowest singlet and triplet $n\pi^*$ states are similar.

Now, are $n\pi^*$ states with highly aromatic residuals normally the T_1 states, while the $\pi\pi^*$ states are the T_1 and S_1 states for those with nonaromatic or antiaromatic residuals? Although some molecules like **3** with aromatic residual have T_1 and S_1 $n\pi^*$ states or **6** with antiaromatic residual have T_1 and S_1 $\pi\pi^*$ states, this is not a general situation and, for instance, **1** has a T_1 state of $\pi\pi^*$ nature and an S_1 state of $n\pi^*$ character. It is worth noting that the order between the lowest $^3n\pi^*$ and $^3\pi\pi^*$ transitions, as well as the type of $^3n\pi^*$ state (B_1 or A_2), are nearly always the same with UDFT and TD-DFT (Tables S24 and S34), with the exception of compounds **1** and **4** for which the order of $^3n\pi^*$ and $^3\pi\pi^*$ transitions are switched. This reveals that the order between the states in most cases does not vary with method and relates to intrinsic (chemical) features. Indeed, one can see that the electronegativity of the heteroatom influences

the order and energy difference between the b_1 and a_2 symmetric π^* orbitals (see below), and consequently, it also has a great impact on the order of the $^3n\pi^*$ and $^3\pi\pi^*$ transitions.

Above, it was hypothesized that a more aromatic residual, leading to stabilization of $^3n\pi^*$, correlates with a lower vertical excitation energy, and *vice versa* for an antiaromatic residual. However, this hypothesis is too simplistic as the vertical energy difference between S_0 and the $^3n\pi^*$ state also depends on the relative energy (and (anti)aromaticity) of the S_0 state. Furthermore, the excitation energy may primarily be related to orbital energy differences between n and π^* orbitals, where especially the energy of the first correlates with the electronegativity of the heteroatom. Indeed, among the five Group A compounds, the two with residuals leaning toward aromaticity (**3** and **4**) are the two with the lowest $E(^3n\pi^*)$ (2.6 and 2.9 eV, respectively) while, thiopyrylium (**6**), with its antiaromatic residual, and the S_0 nonaromatic pyrylium (**5**) have $E(^3n\pi^*)$ of 5.5 and 5.8 eV, respectively. The same relationship is observed for the $^1n\pi^*$ states (3.1 (**3**), 3.8 (**4**), 5.1 (**1**), 5.1 (**2**), and 6.1 eV (**6**)). Clearly, the $E(n\pi^*)$ values vary with the n orbital energies as this orbital is of very low energy for **5** and **6** being HOMO-2 at 2.09 and 1.78 eV below the highest occupied π-orbital (HOMO), but high for **3** and **4** (for **3** it is as much as 1.89 eV above the highest occupied π-orbital which is HOMO-1). Thus, electronegativity variations among the E atoms is the factor that most strongly impacts on $n\pi^*$ excitation energies, yet, as will be seen for Group B compounds, the (anti)aromaticity difference between the S_0 and $n\pi^*$ states explains variations in the excitation energies of isomeric compounds (*e.g.*, the three diazines).

For the $^3n\pi^*$ states, EDDB results (Figure 5A) are consistent with the MCI ones, with the addition that for EDDB it is technically easier to separate σ- and π-contributions. Accordingly, compounds **3** and **4** exhibit π_β-components which are slightly larger than half of the total π-S_0 value, indicating aromatic character of the residuals of their $^3n\pi^*$ states. For the

other Group A compounds, the π_β-component in T_1 is smaller than in S_0. However, if we look at the total $(\sigma+\pi)$ β-components the results differ, especially for **5** and **6**, due to an increase of the delocalization of σ-electrons (see section 2.3 in the ESI for further details). Is it worth mentioning that the contribution of the antiaromatic π_α-component to MCI is close to zero in all cases, whereas EDDB yields one to 1.5 delocalized electrons out of the total four π_α-electrons.
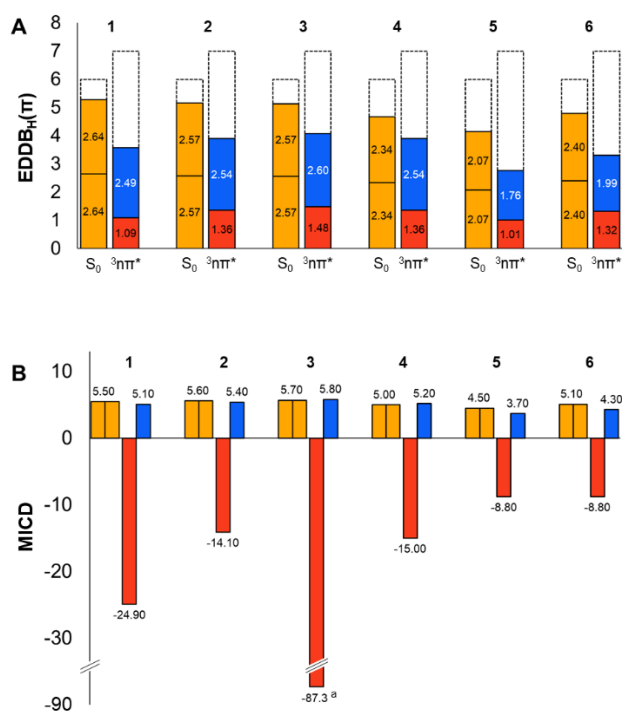
Figure 5: Spin-separated results of Group A heteroaromatics for S_0 and $^3n\pi*$ states; (A) π-EDDB values (units are electrons) at CAM-B3LYP/6-311+G(d,p) level, where red and blue bars correspond to α- and β-electrons, respectively (as references, total π-EDDB values for the aromatic S_0 state of benzene is 5.33 e and for the antiaromatic $^3\pi\pi*$ state of pyridine 2.77 e). The dashed line bars show the total number of π-electron in that state. (B) π-electron bond current strengths (in nA T^{-1}) calculated as the average of all bonds in the given ring at CAM-B3LYP/6-311+G(d,p) level, where red and blue bars correspond to α- and β-electron contributions, respectively.

The trend in the MICD results resembles that for the electronic indices, although the values are markedly offset towards antiaromaticity since the $\pi\alpha$-components give strong paratropic influences. As an illustration, Figure 6 displays the spin separated π-electron MICD maps of the S_0 and $^3n\pi^*$ states of **1**, as well as the orbital transition scheme which provides a qualitative rationalization of the MICD obtained with the CTOCD-DZ methodology.[42,43,44] In S_0, the π-electrons of all Group A compounds induce diatropic currents due to translational transitions between the occupied b_1 and a_2 as well as unoccupied b_1 and a_2 MOs. Completely analogous transitions are found in the $^3n\pi^*$ state within the π_β-electron stack, which gives contributions to diatropic currents. However, the π_α-electrons induce very strong paratropic currents, which arise from the rotational transition from the highest occupied b_1 level to the empty a_2 orbital. Although the α-SOMO-1 (a_2) and α-SOMO-2 (b_1) contribute to diatropic currents through translational transitions to the unoccupied a_2 orbital, these contributions are small in comparison to the paratropic currents involving α-SOMO (b_1). Interestingly, the relative importance of the orbital transitions within the π_α-electron stack was found to be in agreement with the size of the energy gaps between the corresponding orbitals, and these are closely related to the electronegativity of the E atom and not to (anti)aromaticity. Thus, it becomes clear that the magnetic aspect of aromaticity may not agree with the electronic, energetic, and geometric aromaticity aspects, as reported for the $^3\pi\pi^*$ state of $B_4N_4H_8$.[45] A more detailed analysis of the orbital transitions is provided in the ESI (Table S23).
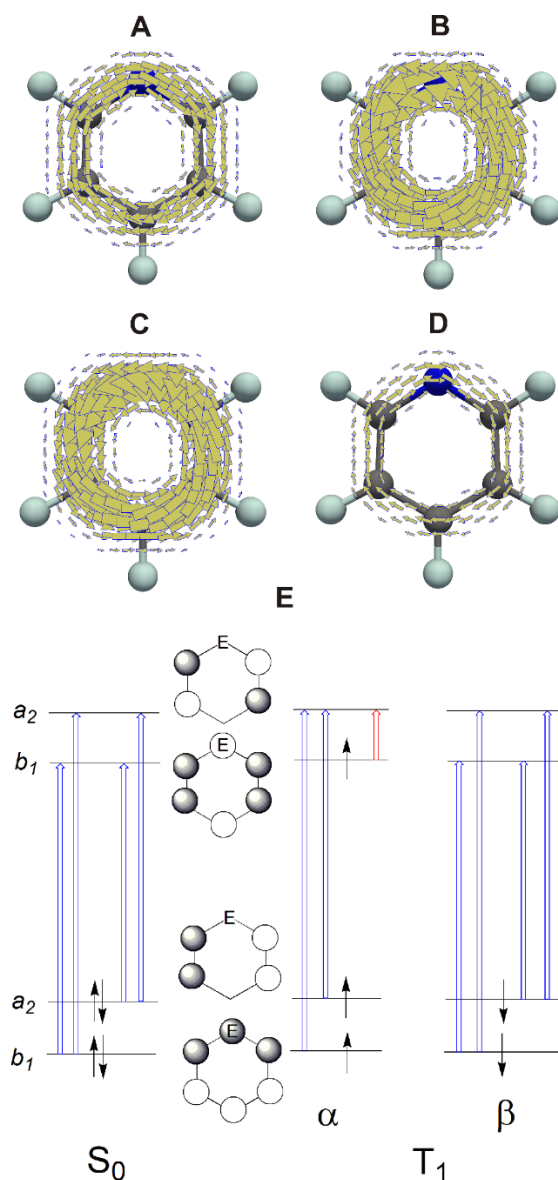
Figure 6. Maps of magnetically induced π-electron current densities calculated 1 bohr above the molecular plane of **1**: (A) S_0 state, (B) $^3n\pi^*$ state, (C) and (D) π_α- and π_β-electron contributions for the $^3n\pi^*$ state. Clockwise (anticlockwise) circulation corresponds to diatropic (paratropic) currents. (E) Qualitative energy level diagram for the frontier molecular orbitals in the S_0 and $^3n\pi^*$ states of Group A. Blue arrows indicate the translationally allowed transitions (inducing diatropic currents), and the red arrow indicates the rotationally allowed transition (inducing paratropic currents). Based on the values of the linear and angular momentum matrix elements, only the most relevant transitions were selected.

Now, what are the reasons for the variation of the (anti)aromatic character of the triplet nπ* states of Group A heteroaromatics? Both the electronegativity of the E atom and the charge of the species play roles as one can see that a low electronegativity of E and a negative charge lead to stronger aromatic character of the residual. The variation can also be due to the local p_π orbital overlap which is differently strong among the Group A compounds. For this reason, we analyzed the degree of uniformity in the π-electron distribution in the ring by calculating the root mean square deviation of π-electron distribution (RMSD(π)) obtained from a natural population analysis (NPA). Interestingly, there are good correlations between the MCI and RMSD(π) for both S_0 and T_1, indicating that the more uniformly distributed the π-electrons, the higher the MCI (Figure S5). It is further notable that there is a reasonable correlation with the change in the RMSD(π) of the π_β-electron distribution when going from S_0 to T_1 and the degree of (anti)aromaticity of the residual, implying that if the π_β-electron distribution becomes more uniformly distributed upon excitation, the residual of the system will become more aromatic, and *vice versa*. This is in line with the observation above that the heteroatom E has an apparent impact on the (anti)aromatic tendency of the residual of vertical nπ* states of Group A heteroaromatics.

Finally, we tested the hypothesis that molecules with aromatic residuals in nπ*, when compared to the S_0 state, remain as modestly distorted as possible at their relaxed geometries. Here, it should, however, be noted that the six Group A compounds constitute a very small set. The only Group A compound with a relaxed T_1 state of pure nπ* character is **3**, and upon relaxation from its vertical ^{3}nπ* state, it shifts to a planar, anti-quinoidal structure. The degree of aromaticity is lowered slightly according to MCI, but remains relatively high. Curiously, this ^{3}nπ* state is the 1^3A_2 state opposite to the lowest vertically excited ^{3}nπ* state which is $^3B_1$. The minimum of the latter state is 0.15 eV higher in energy, and its relaxed structure is puckered but slightly more aromatic according to MCI and HOMA (Tables S8, S27

and S19). Compounds **2**, **5**, and **6** keep planar structures in their relaxed ^{3}nπ* states, however, these states are 1.14 – 3.57 eV above the T$_1$ states which are of ππ* character. Conversely, **1** and **4** pucker in their ^{3}nπ* states and become mixed nπ*/ππ* in character. Thus, the extent of (anti)aromatic character of the residual seems not to explain the puckering or the retention of planarity in the ^{3}nπ* states (for instance, both **3** with an aromatic residual and **5** with an antiaromatic remain planar). Other factors such as the preferred valence angle of a certain E atom or Pauli repulsion should play relevant roles.

Diheteroaromatic 6-MRs (Group B): Incorporation of two heteroatoms into the π-conjugated cycle makes analysis more complex as (*i*) there is a variation in the S$_0$ state aromatic character with the relative positions of the two heteroatoms,[26,27] and (*ii*) with two lone-pairs there are several nπ* states since there are two (near-degenerate) lone-pair orbitals in addition to the two (near-degenerate) π* orbitals. Because of this latter fact, the nπ* states may have multiconfigurational character. There can also be a variation between the heteroaromatics as to which nπ* state is the lowest in energy making a comparison ambiguous (for the D_{2h} symmetric pyrazine the lowest two nπ* states are B_{3u} (Type I) and A_u (Type II)).

To facilitate the analysis, we split the diheteroaromatics of Group B into two subgroups: one subgroup composed of diheteroaromatics with two different heteroatoms (**10 – 14**) and one with those with two equal heteroatoms (**7 – 9** and **15 – 19**). Those with two different heteroatoms should (in theory) have the highest n orbital dominated by the least electronegative element, and their first nπ* state may resemble those of the monoheteroaromatics with the same heteroatom. Yet, we will see that this is not necessarily the case. In our analysis, we calculate MCI throughout the group and MICD for selected compounds. We primarily analyse the vertical ^{3}nπ* states, however, we also explore if they relaxed to (near-)planar structures which remain as ^{3}nπ* states or if they pucker to mixed ^{3}nπ*/ππ* states.

Diheteroaromatic 6-MRs with E' ≠ E: Starting with the three azaphosphorines **10** – **12**, we found that these three species in their T_1 states have values from the T_1 diagnostics at UCCSD(T) level which are above the threshold 0.044 for open-shell species,[39,40,41] indicating multiconfigurational character. For that reason, we also explored these species at UBD and CASSCF levels (see sections 2.1, 3.1 and 3.4 of the Supporting Information), and found that the trend with KS-UDFT agrees with that of UBD.

At UCAM-B3LYP level, there is a minute increase in the aromaticity of the S_0 state according to MCI when going from **10** to **12** while there is a minute aromaticity decrease in the total MCI values of the lowest $^3n\pi^*$ state (Figure 7). The total MCI values of their $^3n\pi^*$ states resemble those of **1** and **2** (Figure 4), however, they have residuals which tend toward antiaromatic character whereby they resemble **1** more than **2**. In contrast to the predictions based on electronegativity, the formal lone-pair orbitals involved in the lowest $^3n\pi^*$ states of **10** – **12** are somewhat more localized on the N atoms than on the P atoms (Figure 8). Furthermore, these orbitals are 1.08 – 1.43 eV higher in energy than those more centred at the P atoms, and this explains the resemblance of the $^3n\pi^*$ states of **10** – **12** to that of **1**.

Above, in the Introduction, we hypothesized that the (anti)aromatic character of the residual and the vertical $E(^3n\pi^*)$ may correlate. Since there is no extensive variation in the (anti)aromatic character in neither the S_0 states of **10** – **12** nor in the residual of their $^3n\pi^*$ states, the variation in their vertical $E(^3n\pi^*)$, which is modest (3.34 – 3.60 eV), is in accordance with that hypothesis. However, it should be noted that there is a variation among **10** – **12** as to which state is T_1 because the lowest vertical $^3n\pi^*$ and $^3\pi\pi^*$ states of **10** and **12** are of very similar energies but for **11** the $^3\pi\pi^*$ state is lower than $^3n\pi^*$ by 0.34 eV. Finally, it is noteworthy that each of the three isomers, in resemblance to pyridine, pucker in their lowest $^3n\pi^*$ state.
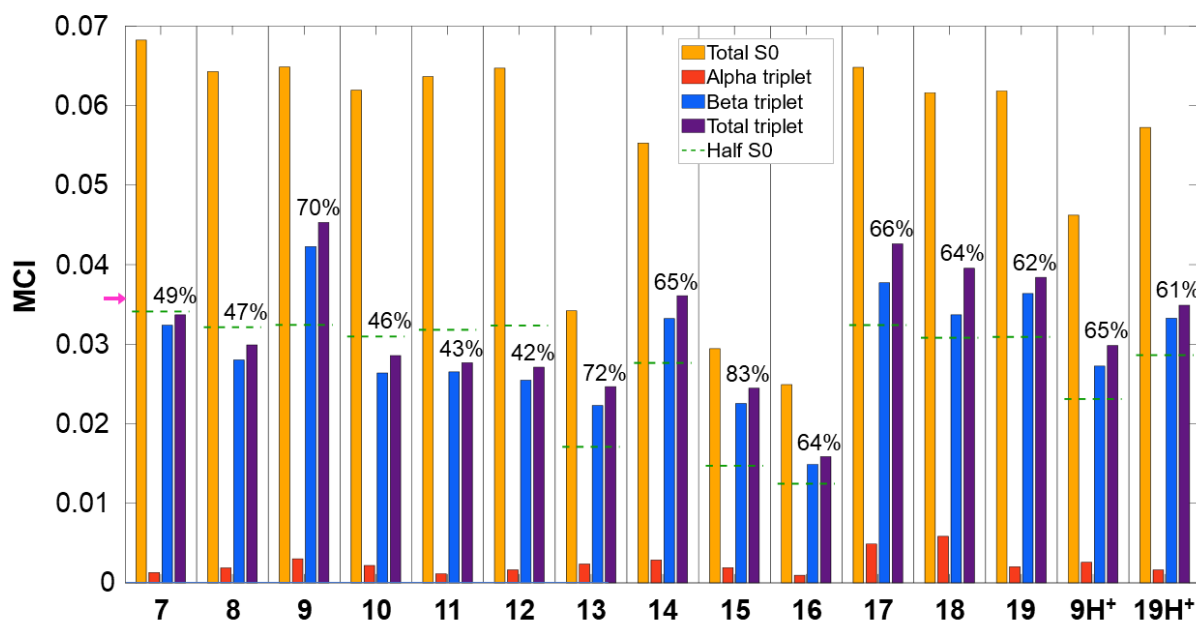
Figure 7: The MCI results (in atomic units) of Group B heteroaromatics in their nπ* triplet states (spin-separated MCI) with UCAM-B3LYP/6-311+G(d,p). A purple arrow indicates half the total MCI value of S_0 benzene, used as an aromaticity threshold.
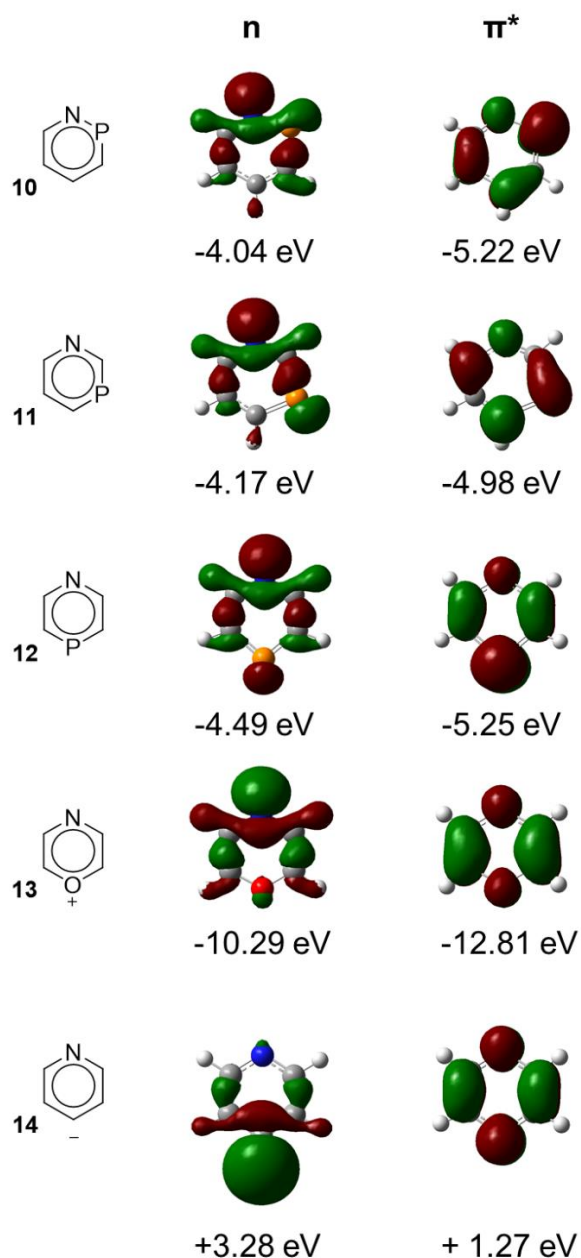
Figure 8: Plots of the n and π* orbitals of **10 – 14**, with orbital energies in eV. Isosurfaces of 0.040 a.u.

Of the two other diheteroaromatics with E ≠ E' (**13** and **14**), it is only **14** that exhibits a sufficiently aromatic character in S_0 to be labelled as aromatic according to our criterion (MCI ≥ 0.0358). The $^3n\pi^*$ state of **14** resembles that of **3**, which means that also this

excitation can be described as that of a monoheteroaromatic. Further support for this interpretation comes from the shape of the formal n orbital involved in the $n\pi^*$ excitation since it has a marked localization at the anionic C atom. With regard to **13**, it has a non-aromatic S_0 state but is still an interesting compound since its MCI value in the $^3n\pi^*$ is significantly higher than half the S_0 value. The total MCI value is intermediate between that of **5** and **1**, and the MCI_β-component suggest that **13** in its lowest $^3n\pi^*$ state leans towards a weak aromatic character. Furthermore, the $^3n\pi^*$ states are the T_1 states of both **13** and **14**, and the n orbitals are heavily localized at the more electropositive of the two heteroatoms in line with the hypothesis above. On the other hand, the extent of aromaticity is determined by the π-orbital overlap, and since O only provides a poor π-overlap it leads to a very significant attenuation of the aromaticity. This shows, as may seem obvious, that the shape of the highest lone-pair orbital and the extent of aromaticity of the $^3n\pi^*$ state are not linked since the lowest $^3n\pi^*$ of **13** resembles that of **1** while at the same time its extent of aromaticity resembles that of **5**.

In many cases, C and P are considered similar in chemical bonding features with P being a "carbon copy".[46] For that reason, is notable that the $^3n\pi^*$ states of **12** and **14** have markedly different (anti)aromatic character, both with regard to the relative value of the residual and the absolute MCI value. This is also reflected in relaxed structures of the (formerly pure) $^3n\pi^*$ states because **14** keeps a near-planar structure while **12** puckers markedly and attains a mixed $^3n\pi^*/\pi\pi^*$ state.

Diheteroaromatic 6-MRs with E' = E: Among these species only **17** and **18** exhibit multireference character, a result which should stem from the near-degeneracy of the two lowest $^3n\pi^*$ states. Results from UBD and CASSCF calculations, however, again corroborate that UCAM-B3LYP provides reliable aromaticity results and trends (Tables S9, S12 and S13).

For the three diazines **7** – **9**, the aromaticity of the S_0 state follows the expected order pyridazine (**7**) > pyrimidine (**8**) ~ pyrazine (**9**).[47] For these species, the lowest $^3n\pi^*$ states are the T_1 states and we find that the excitations are of similar type (Type I) (see Table S28), although a comparison is ambiguous in a strict sense. With regard to aromaticity, MCI values indicate that the $^3n\pi^*$ state of **9** has a residual with clear aromatic character, while **7** and **8** have residuals in line with nonaromatic character (*i.e.*, half of the S_0 values). Interestingly, although the largest difference in the MCI values between **7**, **8** and **9** is due to the MCI_β component, the MCI_α of **9** is also larger than those of **7** and **8**, indicating less strong antiaromatic character in the $^3n\pi^*$ state of **9** than in its two isomers. Furthermore, our finding on the three diazines is in accordance with a recent finding on the lowest excited states of these molecules, yet, where these states were not differentiated as $n\pi^*$ or $\pi\pi^*$ states.[17] It was argued that the more aromatic a molecule is in its S_0 state, the more antiaromatic it will be in its first electronically excited manifolds. Such a relationship was earlier found for the $\pi\pi^*$ states of substituted fulvenes and related hyperconjugated compounds.[48] However, when the states are of different character the relationship does not hold (Figures 4 and 7). For instance, **7** is more aromatic than **8** in both its S_0 and T_1 ($^3n\pi^*$) states.

At this point, one may ask why the $^3n\pi^*$ state of **9** exhibits such a highly aromatic residual? Is it only found with electronic indices or also with magnetic and energetic aromaticity indices? An energy-based evidence of a higher aromatic character of the $^3n\pi^*$ state of **9** when compared to those of **7** and **8** comes from the relative energies in this state because **7** and **8** are higher in energy than **9** by, respectively, 0.21 and 0.34 eV. Additionally, and in agreement with the MCI results, the calculated MICD for **7** – **9** demonstrate that only **9** exhibits a somewhat stronger π_β-electron ring current in its $^3n\pi^*$ state compared to its S_0 state. Moreover, the α-HSOMO of **9** has the least intensive paratropic contribution among **7** – **9**, in accordance with the values of the α-HOMO-LUMO gap (Table S23). Thus, electronic and energetic indicators

support that the $^3n\pi^*$ state of **9** has some aromatic character, and the magnetic indicator reveals that **9** has the least antiaromatic T_1 state among the diazines. In this context it is notable that perfluoropyridazine has been found to photorearrange to the corresponding pyrazine,[29,30] and it has been concluded that these rearrangements occur in the singlet $n\pi^*$ state. Hence, it is rewarding that we find the same trends for the S_1 states of the diazines as for their T_1 states, with **9** being the most stable and aromatic isomer in its $^1n\pi^*$ state.

Further clarity on the cause of the aromatic residual is gained by looking into the distribution of the π-electrons. In the S_0 state, the π-population is more evenly spread in **7**, followed by **9**, and lastly by **8**, in agreement with the results presented in Figure 7. In the $^3n\pi^*$ state, on the other hand, the π-electron distribution in **9** is clearly more uniform than in the other two species due to the high symmetry of the former (see Tables S42-S44). In fact, the π_β-electron population is even more evenly distributed in this state than in the S_0 state, in line with the findings for the MCI$_\beta$-component obtained with the electronic and magnetic aromaticity indices. After excitation to the $^3n\pi^*$ state, there is an accumulation of the excess π_α-electrons around the N atoms. For **7** and **8**, the π_β-electrons are also quite localized in N atoms and in particular C atoms, leading to a less uniform π-electron distribution and the consequent reduction of the aromaticity of the π_β-electrons. In D_{2h} symmetric **9**, despite some accumulation in the N atoms, the distribution of π_β-electrons is forced by symmetry to be more uniform (all C atoms have the same π-electron population), thus explaining the increase in the aromaticity of the MCI$_\beta$-component.

Now, returning to the hypothesis that the (anti)aromaticity difference between S_0 and the $^3n\pi^*$ states of **7** – **9** impacts on the $E(^3n\pi^*)$, the largest difference in (anti)aromaticity is found for **7** while the smallest is found for **9** (Figure 7). However, the simple hypothesis is not valid because **7** has the lowest $E(^3n\pi^*)$ (2.95 eV) and **8** the highest (4.13 eV). Yet, the transition energies are primarily influenced by the relative energies in S_0 because in this state **8**

is more stable than **7** by 1.03 eV (Table S28), a feature that stems from repulsion between the lone-pair electrons of the two adjacent N atoms of **7**.[49]

Among the further compounds with E = E', **15**, **17** and **19** are also special as they have residuals in their $^3n\pi^*$ states with considerable aromatic character. Hence, it is clear that the placement of heteroatoms with in-plane lone-pairs in *para*-positions, leading to D_{2h} symmetric molecules, provides for $n\pi^*$ states with strong aromatic characters of the residuals. Again, it is interesting to compare the relative energies of the isomer pairs in their $^3n\pi^*$ states. In the $^3n\pi^*$ state, isomer **15** with a higher residual than **16** is lower in energy by 0.90 eV but for **17** and **18**, where the difference in the residual is smaller, isomer **18** is lower in energy by 0.14 eV. In S_0, the relative stability of **15** as compared to **16** is opposite to that in the $^3n\pi^*$ state, and as a result, $E(^3n\pi^*)$ is smallest for **15**. For the same reason, **18** is found to have a lower $E(^3n\pi^*)$ than **17**.

One can note that the electronegativity of E impacts on the aromaticity in the S_0 state, and thus, also on the absolute MCI value of the $^3n\pi^*$ state. However, the main factor impacting on the MCI value of the $^3n\pi^*$ state, relative to the S_0 state, is the placement of the heteroatoms as the *para*-isomers always have markedly aromatic residuals. Furthermore, one can note that it is mainly in the MCI_β-components that the increase occurs. One can ask if it is an increased electrostatic repulsion that leads to a distribution of the π_β-electrons among atoms in the 6-MR? Yet, when regarding **9** and **17**, which both are strongly aromatic in S_0 and which also have strong aromatic character of the residual of the $^3n\pi^*$ state, the two species have different π^* orbitals and the $n\pi^*$ states are thus of different types in the two compounds (B_1 in **9** and A_2 in **17**). One may thereby conclude that the type of π^* orbital does not impact on the aromatic character of the residual.

A further item to note is that compounds with electronegative elements, primarily O, being weakly aromatic or nonaromatic in S_0, gain some aromaticity within the MCI_β-component in the $n\pi^*$ state (more than half the value in the S_0 state). These species have rather localized π-electrons in the S_0 state because of the highly electronegative and electron deficient O^+. Yet, upon the $n\pi^*$ excitation the π_β-electrons delocalize due to the addition of one electron to the π system, and we find that the β-components increase both with MCI and MICD.

Finally, for the whole group B, we have also found a good correlation with the change in the $RMSD(\pi)$ of the π_β-electron distribution when going from S_0 to T_1 and the degree of (anti)aromaticity of the residual (Figure S7). In particular, the π-electron distribution in the $n\pi^*$ state of **9** and **15**, which have the heteroatoms located in *para*, is clearly more uniform than in their counterparts due to its higher symmetry.

Protonated para-diheteroaromatics: For the three Group B diheteraromatics with $E = E'$ atoms at *para*-positions and with aromatic S_0 states (**9**, **17**, and **19**) we also explored the changes in (anti)aromatic character upon protonation of their $^3n\pi^*$ states. This leads to **9H$^+$**, **3** and **19H$^+$**, respectively. These three new species remain aromatic in S_0 even though the aromaticity goes down according to MCI in all cases. Importantly though, the residuals of their $^3n\pi^*$ states remain aromatic in character in each of these species, indicating that protonation reduces the aromaticity of both the S_0 and $^3n\pi^*$ states by a similar percentage. However, when **14** is protonated at the negative C atom, leading to **1**, there is no aromatic residual but rather an antiaromatic residual.

***Osmapyridines (Group C)*:** At this point, one may ask if the approach for rationalizing the (anti)aromatic character of $n\pi^*$ states of heteroaromatics can be applied to other compound classes and other excitations? For this reason, we explored the osmapyridines **20** and **21**, which have been found through computations to be aromatic in both S_0 and T_1, a feature which has been labelled as *adaptive aromaticity*. We probe if this feature, observed for

T_1 state being the lowest $^3\pi\sigma^*$ and $^3\sigma\pi^*$ states, can be explained in the framework we put forth herein for the $^3n\pi^*$ states of heteroaromatics. The $^3\pi\sigma^*$ and $^3\sigma\pi^*$ states also have differences in the number of π_α- and π_β-electrons. Thus, the aromaticity observed in the T_1 states of certain metallaaromatics occurs when the residual between the two spin-components is not nil. To explore this, we computed the spin-separate MCI and MICD of two osmapyridines labelled as adaptive aromatic (**20** and **21**),[23] analysing both their vertical and relaxed $^3\sigma\pi^*$ states. Noteworthy, the computed degree of aromaticity for the triplet $\sigma\pi^*$ or $\pi\sigma^*$ states of metallaaromatics labelled as adaptive aromatic is in most cases lower than for the closed-shell singlet state, which resembles what is observed for all heteroaromatics explored above in their $^3n\pi^*$ states when compared to S_0.

Our results for **20** and **21** compare qualitatively with previously reported trends, although our MCI values are lower. Now, based on the criteria set up above, only **21** should be considered to have an aromatic residual (Figure 9). The residual of osmapyridine **20** in $\sigma\pi^*$ instead tends towards antiaromaticity, or alternatively, a non-aromatic character if based on the previously reported MCI results. In both cases, the residual is a result of a very low (negative) MCI_α-component and a higher MCI_β-contribution, with the latter having a greater impact on the residual, similar as for the heteroaromatics.
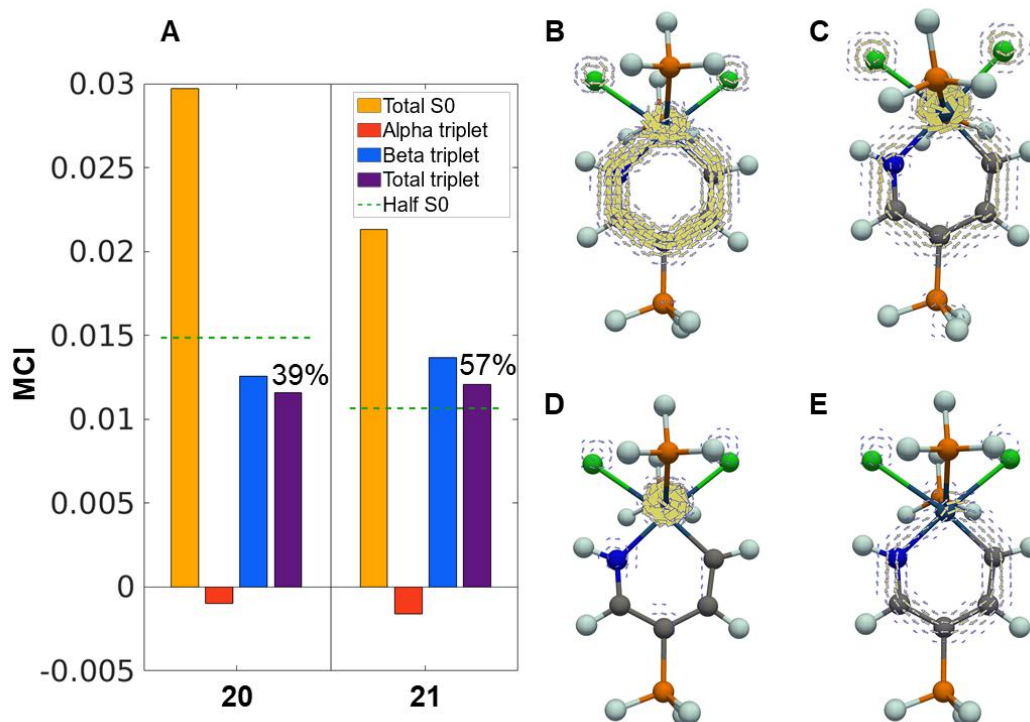
Figure 9: Results on the osmapyridines: (A) the vertically spin-separated MCI values; (B) – (E) π-electron MICD plots calculated 1 bohr above the molecular plane of **21**: S_0 state (B) and vertical $^3\sigma\pi^*$ state (C) with the corresponding π_α- and π_β-electron contributions, (D) and (E). Clockwise circulation corresponds to diatropic (aromatic) currents.

MICD calculations generally support these findings. Both **20** and **21** sustain relatively strong diatropic current densities in the singlet state (Figures 9B and S3A), yet in the $^3\sigma\pi^*$ state of **20** the global circulation practically completely vanishes, in the corresponding state of **21** there are rather weak diatropic currents (Figures 9C and S3B). According to the calculated MICDs, **21** can be considered as aromatic in the singlet state, but only weakly aromatic in the $^3\sigma\pi^*$ state. The aromatic character of **21** in the $^3\sigma\pi^*$ state comes from both the diatropic current density contributions of π_β-electrons and from relatively weak paratropic currents of π_α-electrons. The contribution of π_β-electrons in the $^3\sigma\pi^*$ is less significant than the corresponding one in the singlet state. Therefore, the aromaticity of the singlet **21** is preserved

in the triplet state mainly due to the fact that the α-HSOMO induce very weak paratropic current density contribution, which comes from a relatively large α-HOMO-LUMO gap (Table S23).

Upon geometry relaxation, both compounds in their $^3\sigma\pi^*$ states gain aromaticity according to MCI, and the relaxation energy reflects this change. When vertically excited from the optimal singlet state geometry, the $^3\sigma\pi^*$ states of **20** and **21** are, respectively, 0.64 and 1.06 eV above the S_0 state, but after relaxation this changes to 0.12 and -0.20 eV (Tables S32 and S33), whereby the latter species has a triplet ground state (T_0), in line with previous findings.[23] Interestingly, the aromaticity gain comes about because of two effects (see the ESI, Tables S16 and S17). For **20**, the increase in aromaticity mainly stems from an increased MCI$_\alpha$-component, which means that the relaxation alleviates the antiaromatic π_α-contribution. In **21**, on the other hand, the MCI$_\alpha$-component remains rather unchanged upon geometry relaxation while the aromaticity according to the MCI$_\beta$-component increases significantly.

However, unlike the MCI values, the calculated MICDs are practically insensitive to the effects of the geometry relaxation of the $^3\sigma\pi^*$ state, in line with previous studies showing that MICD is mainly influenced by symmetry and nodal characteristics of the frontier orbitals, and far less by small geometry modifications.[50]

Interestingly, according to MICD the vertically excited $^3\sigma\pi^*$ states of both osmapyridines are even slightly more aromatic than the relaxed ones. A reason for the diatropic ring currents in **20** and **21** comes from a smaller paratropic π_α contribution in their $^3\sigma\pi^*$ states, in contrast to the $^3n\pi^*$ states of the Groups A and B compounds. As the orbital energy gaps between α-HSOMO and α-LUMO are slightly larger (~0.25 a.u.) in the osmapyridines compared to the Groups A and B compounds (0.14 – 0.23 a.u.), there would be larger paratropic contributions in the latter species. However, there should also be additional contributing factors that reduce the paratropicity in **20** and **21**. Thus, the absolute contributions of the spin components vary between electronic and magnetic descriptors.

Thus, it becomes clear from the osmapyridines that the approach of separating the α- and β-spin components of electronic states with different numbers of π_α- and π_β-electrons is a useful approach for analysis of the (anti)aromatic character of such states. It provides an overarching theoretical framework to rationalize computational observations on such states.

Conclusions and Outlook

We explored the nπ* states of heteroaromatics with $(4n+2)\pi$-electrons and in-plane lone-pair electrons (*e.g.*, pyridine and the pyrylium ion), and applied Mandado's $2n+1$ rule for aromaticity of separate spins in our analysis. In their nπ* states, these species have $2n+2$ π_α-electrons and $2n+1$ π_β-electrons, which leads to a tug-of-war between the antiaromatic π_α-component and the aromatic π_β-component. Which component is dominant varies between the various heteroaromatics and with different aromaticity descriptors, and we explore if the residuals between the two components lean towards aromaticity or towards antiaromaticity. Yet, can the observations made herein be connected to a coherent pattern?

We first note that for 5-MR heteroaromatics (*e.g.*, thiophene and imidazole) the nπ* states lie far above the lowest excited states. Therefore, the 5-MR heteroaromatics were not considered in detail as their excited state properties which are photochemically relevant are determined by the ππ* state. We instead focus on 6-MRs heteroaromatics with one or two heteroatoms. We find that several heteroaromatics are quite aromatic in their nπ* states, in most cases resulting from an increase in the aromaticity of the β-component when compared to the β-component of the Hückel-aromatic S_0 state. We observed similar trends in the (anti)aromatic character of the residuals when we analyze the magnetically induced current densities (MICD) as with the electronic MCI and EDDB indices. However, the antiaromatic character of the α-component is much more dominant in the MICD results than in the results with the electronic indices.

In general, the (anti)aromatic character of the residual is the same for singlet and triplet $n\pi^*$ states. The heteroaromatic compounds that are likely to exhibit strong aromatic characters of their lowest $n\pi^*$ states, *i.e.*, a residual that leans toward aromaticity, are molecules with high symmetry and with less electronegative heteroatoms.

Although the excitation energies of the $n\pi^*$ states depend on several factors of both the S_0 and $n\pi^*$ states, the relative energies of the $n\pi^*$ states of isomeric heteroaromatics vary in dependence of the aromatic character of the residuals. For example, the $n\pi^*$ state of pyrazine has a residual which is more aromatic than the $n\pi^*$ state of pyridazine, and the first of these diazines is lower than the second one by 0.34 eV. Experimentally one has observed photochemical rearrangements of the perfluorinated pyridazine to pyrazine, concluded to proceed in the $n\pi^*$ state.[29,30] The same applies to the geometric relaxation of the $n\pi^*$ state, this depends on a number of factors where the aromatic character of the residual is only one of the factors.

Finally, we have shown that the situation described here for $n\pi^*$ states of heteroaromatics can extrapolated to understand the aromatic character of some transition metal complexes in their triplet $\sigma\pi^*$ and $\pi\sigma^*$ states, the so-called adaptive aromaticity.[22-25] Not only that but also our analysis can be extended to π-conjugated radical anions and cations such as $C_6H_6^+$ or $C_8H_8^-$ with an even number of π_α-electrons and an odd number of π_β-electrons or vice versa. Indeed, some of these radical cations or anions were already analyzed by Mandado and co-workers who found that in these systems the π_α-component was antiaromatic and the π_β aromatic, or the other way around. However, the authors did not discuss the character of the residuals.[18] As a whole, we think that our findings have significant implications for the understanding the aromatic character any system with $N_\alpha = N_\beta \pm 1$ electrons.

Acknowledgements

References

1 Balaban, A. T.; Oniciu, D. C.; Katritsky, A. R., Aromaticity as a Cornerstone of Heterocyclic Chemistry, *Chem. Rev.* **2004**, *104*, 2777-2812.

2 Baumann, M.; Baxendale, I. R.; Ley, S. V.; Nikbin, N., An Overview of the Key Routes to the Best Selling 5-Membered Ring Heterocyclic Pharmaceuticals, *Beilstein J. Org. Chem.* **2011**, *7*, 442-495.

3 Beverina, L.; Pagini, G. A., π-Conjugated Zwitterions as Paradigm of Donor–Acceptor Building Blocks in Organic-Based Materials, *Acc. Chem. Res.* **2014**, *47*, 319-329.

4 Luo, D.; Jang, W.; Babu, D. D.; Kim, M. S.; Wang, D. H.; Kyaw, A. K. K. Recent Progress in Organic Solar Cells Based on Non-Fullerene Acceptors: Materials to Devices, *J. Mater. Chem. A* **2022**, *10*, 3255-3295.

5 Chen, X.; Tan, D.; Yang, D.-T., Multiple-Boron–Nitrogen (multi-BN) Doped π-Conjugated Systems for Optoelectronics, *J. Mater. Chem. C*, **2022**, *10*, 13499-13532.

6 Huang, J.; Yu, G. Structural Engineering in Polymer Semiconductors with Aromatic N-Heterocycles, *Chem. Mater.* **2021**, *33*, 1513-1539.

7 Lamberth, C. Heterocyclic Chemistry in Crop Protection, *Pest Manag. Sci.* **2013**, *69*, 1106-1114.

8 Lambert, C.; Dinges, J. Eds. Bioactive Heterocyclic Compound Classes: Agrochemicals, Wiley-VCH Verlag Gmbh & Co, 2012, Weinheim, Germany.

9 Baird, N. C., Quantum Organic Photochemistry. II. Resonance and Aromaticity in the Lowest $^3\pi\pi^*$ State of Cyclic Hydrocarbons, *J. Am. Chem. Soc.* **1972**, *94*, 4941-4948.

10 Ottosson, H., Organic Photochemistry: Exciting Excited-State Aromaticity, *Nat. Chem.* **2012**, *4*, 969-971.

11 Karas, L.; Wu, J. I.; Aromaticity: Baird's Rules at the Tipping Point, *Nat. Chem.* **2022**, *14*, 723-725.

12 Rosenberg, M.; Dahlstrand, C.; Kilså, K.; Ottosson, H., Excited State Aromaticity and Antiaromaticity: Opportunities for Photophysical and Photochemical Rationalizations, *Chem. Rev.* **2014**, *114*, 5379-5425.

13 Papadakis, R.; Ottosson, H., The excited state antiaromatic benzene ring: a molecular Mr Hyde? *Chem. Soc. Rev.* **2015**, *44*, 6472-6493.

14 Oh, J.; Sung, Y. M.; Hong, Y.; Kim, D., Spectroscopic Diagnosis of Excited-State Aromaticity: Capturing Electronic Structures and Conformations upon Aromaticity Reversal *Acc. Chem. Res.* **2018**, *51*, 1349-1358.

15 Liu, C.; Ni, Y.; Lu, X.; Li, G.; Wu, J. Global Aromaticity in Macrocyclic Polyradicaloids: Hückel's Rule or Baird's Rule? *Acc. Chem. Res.* **2019**, *52*, 2309-2321.

16 Kim, J.; Oh, J.; Osuka, A.; Kim, K., Porphyrinoids, a Unique Platform for Exploring Excited-State Aromaticity, *Chem. Soc. Rev.* **2022**, *51*, 268-292.

17 Solà, M., Aromaticity Rules, *Nat. Chem.* **2022**, *14*, 585-590.

18 Mandado, M.; Graña, A. M.; Pérez-Juste, I., Aromaticity in Spin-Polarized Systems: Can Rings be Simultaneously Alpha Aromatic and Beta Antiaromatic? *J. Chem. Phys.* **2008**, *129*, 164114.

19 Valiev, R. R.; Kurten, T.; Valiulina, L. I.; Ketkov, S. Yu.; Cherepanov, V. C.; Dimitrova, M.; Sundholm, D., Magnetically Induced Ring Currents in Metallocenothiaporphyrins, *Phys. Chem. Chem. Phys.* **2022**, *24*, 1666-1674.

20 Pedersen, J.; Mikkelsen, K. V., A Benchmark Study of Aromaticity Indexes for Benzene, Pyridine, and the Diazines - II. Excited State Aromaticity *J. Phys. Chem. A*, **2022**, *127*, 122-130.

21 Feixas, F.; Poater, J.; Matito, E.; Solà, M. Aromaticity of Organic and Inorganic Heterocycles, in Structure, Bonding and Reactivity of Heterocyclic Compounds, 2014, Springer Verlag, Berlin.

22 Chen, D.; Shen, T.; An, K.; Zhu, J. Adaptive aromaticity in S_0 and T_1 states of pentalene incorporating 16 valence electron osmium. *Commun. Chem.* **2018**, *1*, 18.

23 Shen, T.; Chen, D.; Lin, L.; Zhu, J. Dual Aromaticity in Both the T_0 and S_1 States: Osmapyridinium with Phosphonium Substituents, *J. Am. Chem. Soc.* **2019**, *141*, 5720–5727.

24 Chen, D.; Szczepanik, D. W.; Zhu, J.; Solà, M. Probing the Origin of Adaptive Aromaticity in 16-Valence-Electron Metallapentalenes, *Chem. Eur. J.* **2020**, *26*, 12964-12971.

25 You, F.; Qui, R.; Zhu, J., Adaptive Aromaticity in Osmapentalene and Osmapyridinium Complexes with Carbone Ligands, *J. Phys. Org. Chem.* **2023**, *36*, e4450.

26 Dey, S.; Manogaran, D.; Manogaran, S.; Schaefer III, H. F., Quantification of Aromaticity of Heterocyclic Systems Using Interaction Coordinates, *J. Phys. Chem. A*, **2018**, *122*, 6953-6960.

27 Feixas, F.; Matito, E.; Poater, J.; Solà, M., On the Performance of Some Aromaticity Indices: A Critical Assessment Using a Test Set, *J. Comp. Chem.* 2008, **29**, 1543-1554.

28 Flicker, W. M.; Mosher, O. A.; Kuppermann, A. Electron Impact Investigation of Electronic Excitations in Furan, Thiophene, and Pyrrole, *J. Chem. Phys.*, **1976**, *64*, 1315-1321.

29 Allison, C. G.; Chambers R. D.; Cheburkov, Yu. A.; MacBride, J. A. H.; Musgrave, W. K. R. J. The Isomerisation of Perfluoropyridazines to Perfluoropyrimidines and to Perfluoropyrazines, *J. Chem. Soc. D*, **1969**, 1200-1201.

30 Johnson, D. W.; Austel, V.; Feld, R. S.; Lemal, D. M. The Pyridazine-Pyrazine Photorearrangement, *J. Am. Chem. Soc.* **1970**, *92*, 7505-7506.

31 Yanai, T.; Tew, D. P.; Handy, N. C. A new hybrid exchange–correlation functional using the Coulomb-attenuating method (CAM-B3LYP). *Chem. Phys. Lett.* **2004**, *393*, 51-57.

32 Becke, A. D. Density-functional thermochemistry. III. The role of exact exchange. *J. Chem. Phys.* **1993**, *98*, 5648-5652.

33 Stephens, P. J.; Devlin, F. J.; Chabalowski, C. F.; Frisch, M. J., Ab Initio Calculation of Vibrational Absorption and Circular Dichromism Spectra Using Density Functional Force Fields, *J. Phys. Chem.* **1994**, *98*, 11623-11627.

34 Becke, A. D. Density-functional exchange-energy approximation with correct asymptotic behavior, *Phys. Rev. A* **1988**, *38*, 3098-3100.

35 Bultinck, P.; Ponec, R.; Van Damme, S. Multicenter bond indices as a new measure of aromaticity in polycyclic aromatic hydrocarbons, *J. Phys. Org. Chem.* **2005**, *18*, 706-718.

36 Feixas, F.; Matito, E.; Poater, J.; Solà, M. Quantifying Aromaticity with Electron Delocalisation Measures, *Chem. Soc. Rev.* **2015**, *44*, 6434-6451.

37 Szczepanik, D. W. A new perspective on quantifying electron localization and delocalization in molecular systems, *Comput. Theor. Chem.* **2016**, *1080*, 33-37.

38 D. W. Szczepanik, M. Andrzejak, J. Dominikowska, B. Pawełek, T. M. Krygowski, H. Szatylowicz, M. Solà, The electron density of delocalized bonds (EDDB) applied for quantifying aromaticity, *Phys. Chem. Chem. Phys.* **2017**, *19*, 28970-28981.

39 Lee, T. J., Taylor, P. R., A diagnostic for determining the quality of single-reference electron correlation methods, *Int. J. Quant. Chem.* **1989**, *36*, 199-207.

40 Jayatilaka, D.; Lee, T. J., Open-shell coupled-cluster theory, *J. Chem. Phys.* **1993**, *98*, 9734-9747.

41 Rienstra-Kiracofe, J. C.; Allen, W. D.; Schaefer III, H. F., The $C_2H_5 + O_2$ Reaction Mechanism: High-Level ab Initio Characterizations, *J. Phys. Chem. A* **2000**, *44*, 9823-9840.

42 Keith, T. A.; Bader, R. F. W. Calculation of Magnetic Response Properties Using a Continuous Set of Gauge Transformations. *Chem. Phys. Lett.* **1993**, *210*, 223–231.

43 Keith, T. A.; Bader, R. F. W. Topological Analysis of Magnetically Induced Molecular Current Distributions. *J. Chem. Phys.* **1993**, *99*, 3669–3682.

44 Lazzeretti, P.; Malagoli, M.; Zanasi, R. Computational Approach to Molecular Magnetic Properties by Continuous Transformation of the Origin of the Current Density. *Chem. Phys. Lett.* **1994**, *220*, 299–304.

45 Preethayalam, P.; Proos Vedin, N.; Radekovic, S.; Ottosson, H. Azaboracyclooctatetraenes reveal that the different aspects of triplet state Baird-aromaticity are nothing but different, *J. Phys. Org. Chem.* **2023**, *36*, e4455.

46 Dillon, K. B.; Mathey, F.; Nixon, J. F. Phosphorus: The Carbon Copy: From Organophosphorus to Phospha-organic Chemistry, Wiley, Chichester, 1998.

47 Mandado, M.; Otero, N.; Mosquera, R. A., Local Aromaticity Study of Heterocycles Using *n*-Center Delocalization Indices: The Role of Aromaticity on the Relative Stability of Position Isomers, *Tetrahedron*, **2006**, *62*, 12204-12210.

48 Jorner, K.; Emanuelsson, R.; Dahlstrand, C.; Tong, H.; Denisova, A. V.; Ottosson, H. Impact of Ground- and Excited-State Aromaticity on Cyclopentadiene and Silole Excitation Energies and Excited-State Polarities, *Chem. Eur. J.* **2014**, *20*, 9295 – 9393.

49 El-Hamdi, M.; Tiznado, W.; Poater, J.; Solà, M. An Analysis of the Isomerization Energies of 1,2-/1,3-Diazacyclobutadiene, Pyrazole/Imidazole, and Pyridazine/Pyrimidine with the Turn-Upside-Down Approach *J. Org. Chem.* **2011**, *76*, 8913-8921.

50 Havenith, R. W. A.; Jenneskens, L. W.; Fowler, P. W. Ring currents that survive bond alternation in constrained 8π and 6π monocycles, *Chem. Phys. Lett.*, **2003**, *367*, 468-474.

For Table-of-Contents use

Aromaticity of nπ^*states